Dye-sensitized TiO_2 nanotube membranes act as visible-light switchable diffusion gate

Electronic Supplementary Information

Imgon Hwang,[1] Francesca Riboni,[1,2] Ekaterina Gongadze,[3] Aleš Iglič,[3,4] JeongEun Yoo,[1] Seulgi So,[1,#] Anca Mazare,[1] Patrik Schmuki[1,2,5]*

[1]Department of Materials Science WW4-LKO, University of Erlangen-Nuremberg, Martensstrasse 7, 91058 Erlangen, Germany

[2]Regional Centre of Advanced Technologies and Materials, Šlechtitelů 27, 78371 Olomouc, Czech Republic

[3] Laboratory of Biophysics, Faculty of Electrical Engineering, University of Ljubljana, Tržaška 25, SI-1000 Ljubljana, Slovenia

[4]Laboratory of Clinical Biophysics, Faculty of Medicine, University of Ljubljana, Zaloška 9, SI-1000 Ljubljana, Slovenia

[5]Department of Chemistry, Faculty of Science, King Abdulaziz University, P.O. Box 80203, Jeddah 21569, Saudi Arabia

Current address: POSCO Technical Research Laboratories, Automotive Steel Surface Research Group

*Corresponding author. E-mail: schmuki@ww.uni-erlangen.de

Anodic TiO_2 nanotube membrane fabrication 2
Control experiments 3
Permeability experiments, dye-sensitized tube membrane and the role of Ag^+ 3
TiO_2 nanotubular layer on Ti foil 5
The role of N719 on polystyrene nanosphere diffusion gating 6
Figures 7
Figure S1 8
Figure S2 9
Figure S3 10
Figure S4 11
Figure S5 12
References 13

Anodic TiO_2 nanotube membrane fabrication

~ 15 μm long nanotubes were first grown by anodizing a Ti foil for 10 min at 120 V.[1–4] Key to such high-voltage and fast anodization is the presence of lactic acid (LA) in the electrolyte:[1,3] LA is known to shift the oxide breakdown voltage in the anodic direction and, by supporting a high ion flux through the oxide film, allows establishing a ultrafast NT growth under self-organizing conditions.[4,5] Remarkably, in view of membrane fabrication and use in a flow-through configuration, a further significant advantage of LA tubes compared to more traditional anodic NTs (*e.g.*, grown in most typical ethylene-glycol based electrolyte[6]) is their superior mechanical resistance that allows fabricating both-end-open membranes with no morphological damage over the entire surface area and thickness.[2,4]

Low-temperature (250°C) air-annealing for 1h of as-formed LA tubes led to a partial crystallization of the amorphous layer, and was followed by a second anodization performed under similar experimental conditions used for the first step. Such double-anodization approach allowed for the growth of two distinct NT layers – *i.e.*, NTs fabricated during the (shorter) second anodization are thinner than those from the first anodization. Finally, dipping the anodic layers in a H_2O_2 aqueous solution under most optimized conditions[4] led to the preferential dissolution of the thin NT underlayer (that is, the tube layer formed during the second anodization step could be more rapidly (and completely) dissolved during mild etching in H_2O_2 solution), resulting in the detachment of 15 μm thick nanotubes (from the first anodization step), in the form of a free-standing and crack-free TiO_2 tube membrane, as shown by SEM images in Figure 1 (main text).

Control experiments

In order to clarify the contribution of different factors to the light-modulated gating properties of flow-through anodic TiO_2 tube membranes, a series of additional control experiments was performed.

Permeability experiments, dye-sensitized tube membrane and the role of Ag^+

The permeability of the NT membrane to N719 molecules was first tested in the dark by measuring the concentration of the dye in both cell compartments (black lines, Figure S2(a)). The decrease of N719 concentration in the "dye solution" side (chamber A), and its corresponding increase in the "reference solution" side (chamber B), show that N719 molecules diffuse through the NT membrane from the higher dye concentration side (A) to the lower concentration side (B), until an equilibrium state is achieved, after *ca*. 7 hours. In line with spectrometric quantitative data, pictures of the experimental set-up at different times (t = 1h, 4h and 8h) illustrate the solution color change associated to dye diffusing through the membrane (Figure S2(b–d)).

Dye-sensitization of a TiO_2 tube membrane was performed by dipping a fresh TiO_2 crystalline NT membrane layer in a 300 μM solution of the Ru-based dye in a mixture of acetonitrile and *tert*-butyl alcohol (volume ratio, 1:1). The membrane was dye-sensitized by dipping for 8 hours. In line with a most standard procedure for preparing dye-sensitized TiO_2 layers for DSSC (dye-sensitized solar cell),[7] this led to dye adsorption on the tube surface. After dye-sensitization, the sample was rinsed with acetonitrile to remove the non-chemisorbed dye.

When in a flow-through configuration, *i.e.*, for the visible light-modulated diffusion of N719 molecules, we observed that using a pre-sensitized or not sensitized TiO_2 tube membrane did not significantly differ in the effect on the kinetic transport of dye through the membrane and its switchability. As shown in Figure S3(a), comparable dye flow-through diffusion trends were

indeed observed with a fresh and a pre-sensitized tube membrane that led to the conclusion that dye adsorption during diffusion does not represent a limiting kinetic factor to the permeability performance of TiO_2 NT membranes.

We also investigated the effect induced by Ag^+ ions in solution on both the dark and the light-modulated NT membrane permeability. In particular, we observed that dark dye diffusion in a Ag^+–free solution is comparable to that measured in the presence of Ag^+ (Figure S3(b)). In other words, Ag^+ ions do not affect the rate of the concentration gradient-driven dye diffusion.

Nevertheless, under light irradiation (λ = 532 nm), the trend of dye concentration in a Ag^+–free environment dramatically changes (Figure S3(c)): a significantly faster decrease of [N719] is observed in compartment A compared to the dark experiment (black line), with no equivalent increase being correspondingly observed in compartment B. This can be ascribed to a photo-promoted dye degradation effect: while diffusing through the membrane, N719 is photo-excited (λ = 532 nm) and generates e^-/h^+ pairs in its LUMO/HOMO levels, respectively.[8,9] An ultrafast injection ($k_{inj} > 3 \times 10^{12}$ s^{-1})[10] of photopromoted electrons into the conduction band (CB) of TiO_2 follows, enabled by the strong coupling between the π^* excited states of the dye and the unoccupied states of TiO_2.[10–12] A driving force of ~ 0.3 eV has been calculated for such process (*i.e.*, N719 π^* orbitals lie ~ 0.3 eV above the unoccupied states of TiO_2)[13] that leads to the photo-oxidation of N719,[12] and therefore to a decrease of the dye overall concentration (low panel, Figure S3(c)). Clearly, at 532 nm any direct contributions from TiO_2 to the photodegradation effect is excluded ($E_{g,TiO2}$ ~ 3.2 eV[14]).

We therefore attribute the photo-degradation inhibition observed while diffusing N719 under light and with $AgNO_3$ (Figure 2 in the main text, and Figure S2(a)), to the presence of Ag^+ in solution. We propose that silver ions in solution can be reduced to metallic Ag^0 by photopromoted N719 e^-. Particularly, in our configuration photopromoted electrons are either

injected first to TiO_2 CB (from N719 LUMO level) and afterwards reduce Ag^+ to Ag^0, or directly injected from the LUMO level of the dye to Ag^+.[15] Metallic Ag has been previously reported to coordinate NCS ligands.[16] Notoriously, N719 molecules are anchored on TiO_2 surface through $–COO^–$ groups,[17] with this adsorption geometry leaving free NCS ligands,[16] that are likely available for the formation of Ag^0–thiocyanate coordinates.[16,18,19] In addition, on the ground of NCS ability of promoting ligand-to-metal charge transfer (LMCT),[10,20] we assume that a *back* electron transfer from (NCS-coordinated) metallic Ag to Ru(III) may occur that eventually regenerates the oxidized dye (*i.e.*, reduces Ru(III) back to Ru(II)). In line with this, we observed that in the presence of Ag^+ no net photodegradation of N719 occurs that competes with its diffusion through the tube membrane (Figure 2(b)).

TiO_2 nanotubular layer on Ti foil

Aiming at excluding any effects related to the trans-membrane ion/particle transport, that is, any artifacts that may be due to the use of a TiO_2 tube membrane, we performed light-assisted experiments similar to those reported in the main text in a more conventional configuration, that is by using a TiO_2 NT (on metal substrate) array (Figure S6).[21]

Irradiating at 532 nm the dye solution in the presence of TiO_2 NTs led to N719 photo-oxidation due to photo-excited $e^–$ injection from the dye to the semiconductor (green line, Figure S6(a)).[9,11,12] However, in line with the results obtained with tube membranes (Figure 2(b) and S2), no (significant) dye photodegradation was observed also in the NT experiments upon the addition of Ag ions (red line, Figure S6(a)) – remarkably, the photostability of N719 is further confirmed by a similar kinetic trend observed for the N719/tube-on-foil experiment under dark conditions, where clearly any light-induced effect could be excluded (black line in Figure S6(a)).

For a more extended proof of concept, we further tested the photostability of the N719/TiO_2 system in a most typical DSSC-like electrolyte composition, that is, by adding an excess amount of I^-/I_2 to the dye (*t*-BuOH/acetonitrile) solution.[17]

According to classic DSSC operating principles:[12,22]

$$dye + h\nu \rightarrow dye^* \quad (1)$$

$$dye^* \rightarrow dye^+ + e^-(TiO_2) \quad (2)$$

$$dye^+ + 3/2\ I^- \rightarrow dye + \tfrac{1}{2}\ I_3^- \quad (3)$$

upon dye visible light-excitation (1) and injection of photopromoted e^- into TiO_2 CB (2), I^- reduces photo-oxidized N719 molecules (dye^+), that is, I^- acts as electron donor and reduces Ru(III) in the oxidized molecular dye back to Ru(II).

In line with this well-established dye regeneration mechanism, we observed no dye photodegradation when the N719/TiO_2 NT system was illuminated in the presence of iodide, and attributed this effect to the hole-scavenging ability of I^- (3) – in a DSSC configuration, upon reaction (3), I_3^- is finally reduced back to I^- by electrons from Pt cathode.[17]

The role of N719 on polystyrene nanosphere diffusion gating

Experimental evidence of the proposed light- and charge-gated mechanism for NP diffusion through the tube membrane was obtained by measuring the polystyrene permeability in the absence of N719 in the diffusing medium (Figure S5): when the nanosphere/tube membrane arrangement was irradiated in the absence of dye, no significant change in NP concentration was observed; in other words, in the absence of a visible light-responsive moiety (*i.e.*, the dye) the flow-through membrane is in a gate-off state that prevents polystyrene nanosphere from diffusing. Also, the hindered kinetics of NP light-diffusion in the absence of N719 matches the dark diffusion, yet with N719 in solution.

Figures

Figure S1

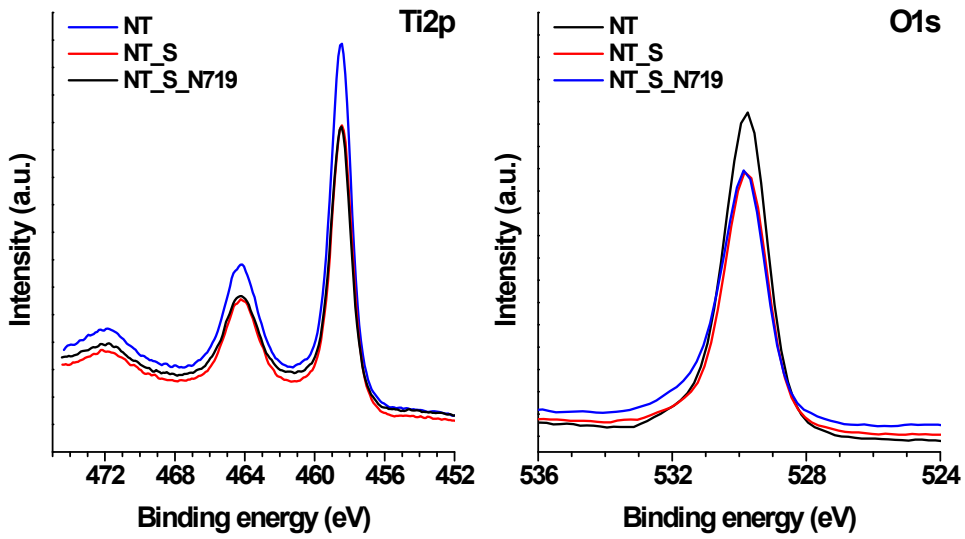

Figure S1. High resolution XPS spectra of Ti2p and O1s peaks for bare nanotubes (NT), nanotubes immersed in solution without dye (NT_S) and nanotubes immersed in the dye solution (NT_S_N719).

Figure S2

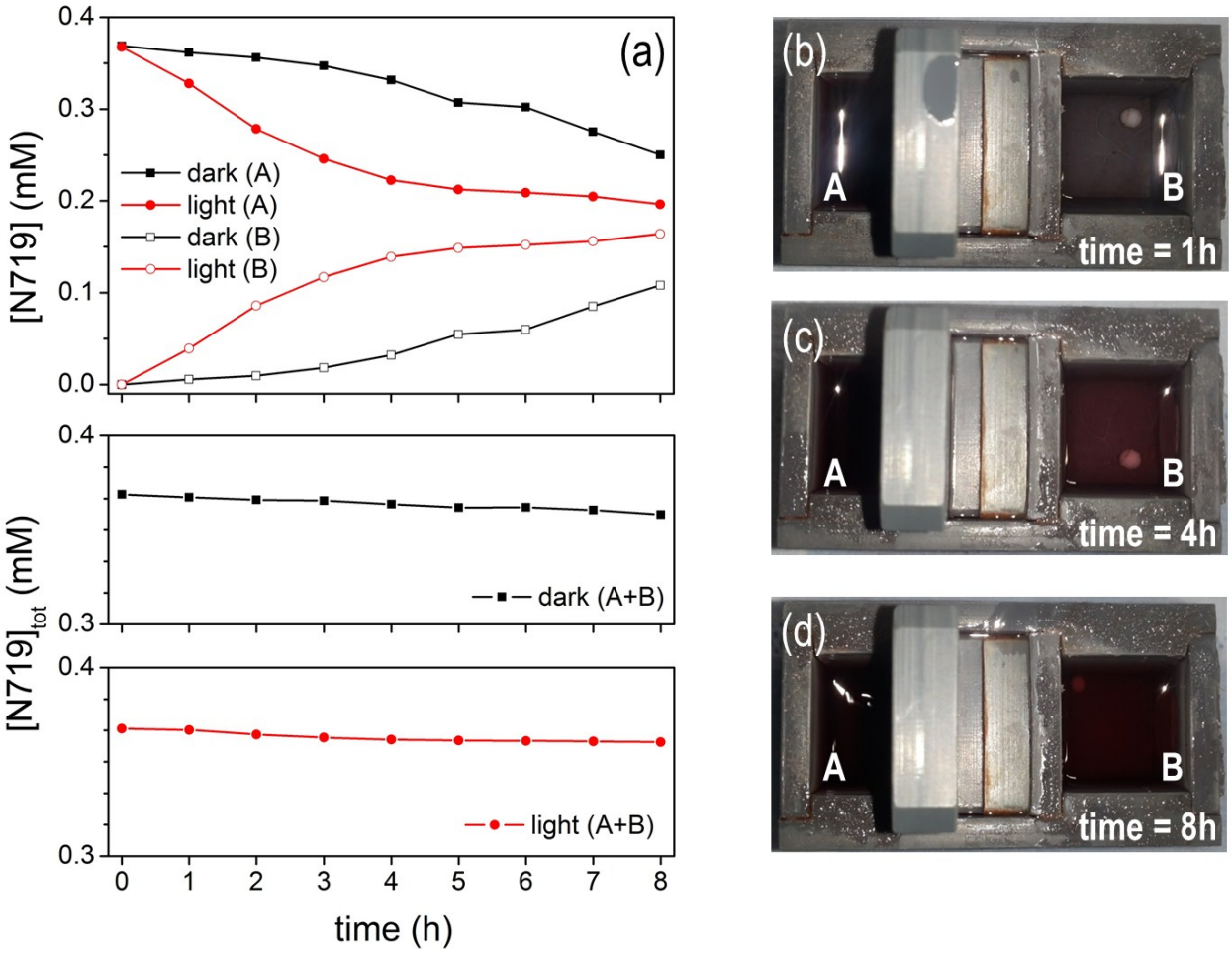

Figure S2. (a) Upper panel: kinetics of dye diffusion in the presence of Ag^+ ions, measured in the dark (black plots) and under 532 nm irradiation (red plots). Middle and lower panels: total (side A + side B) dye concentration measured in the dark and under light, respectively. (b–d) Optical images taken at different times of the reactor during dye permeation, in the presence of Ag^+ ions, through a TiO_2 gating membrane.

Figure S3

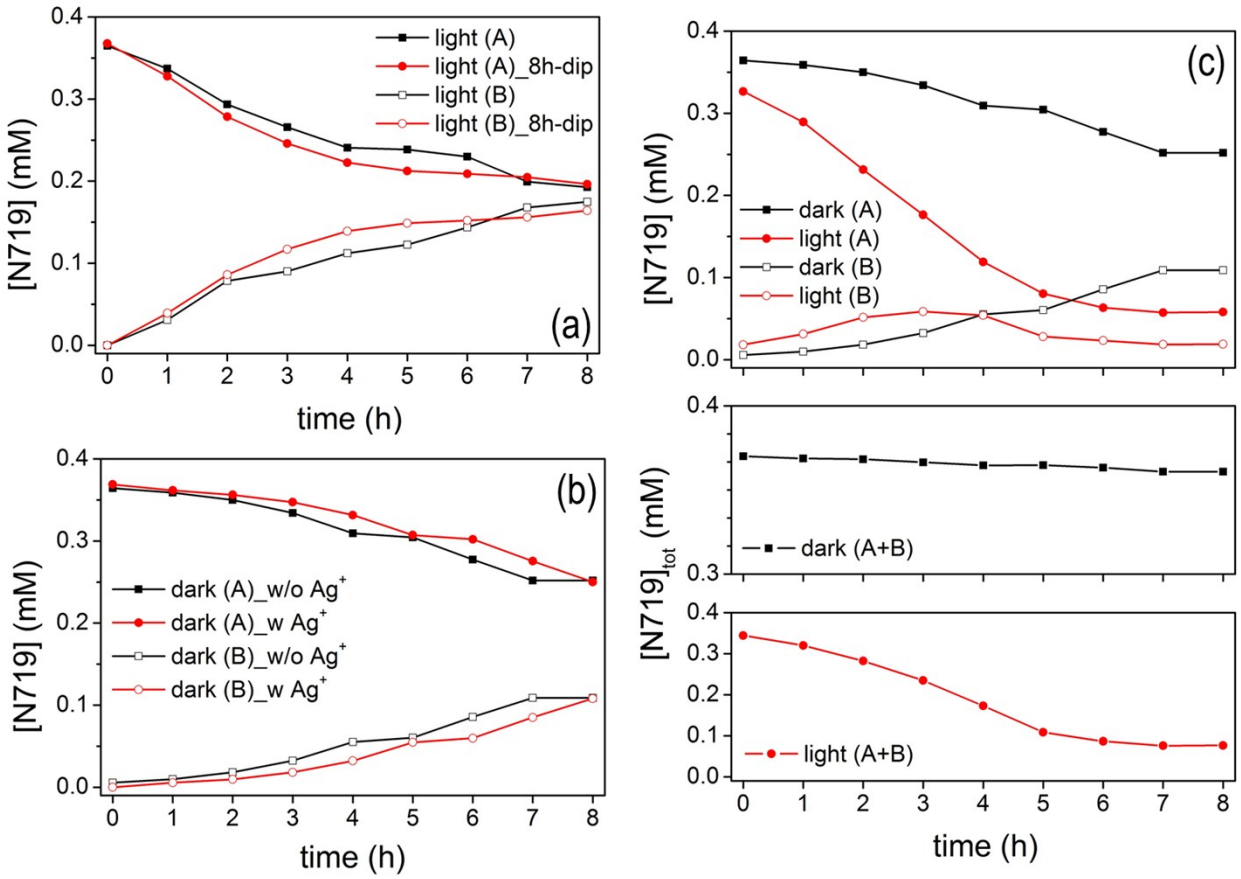

Figure S3. (a) Kinetics of dye diffusion in the presence of N719 and under 532 nm irradiation, measured with a fresh membrane (black plots) and with a dye-sensitized membrane, that is, used after 8h dipping in a N719 dye solution (red plots). (b) Dye diffusion in the dark in the absence (black plots) and presence (red plots) of Ag^+. Ag^+ ions do not affect the kinetics of N719 permeability through the membrane. (c) Upper panel: kinetics of dye diffusion in the absence of Ag^+ ions, measured in the dark (black plots) and under 532 nm irradiation (red plots). Middle and lower panels: total (side A + side B) dye concentration measured in the dark and under light, respectively.

Figure S4

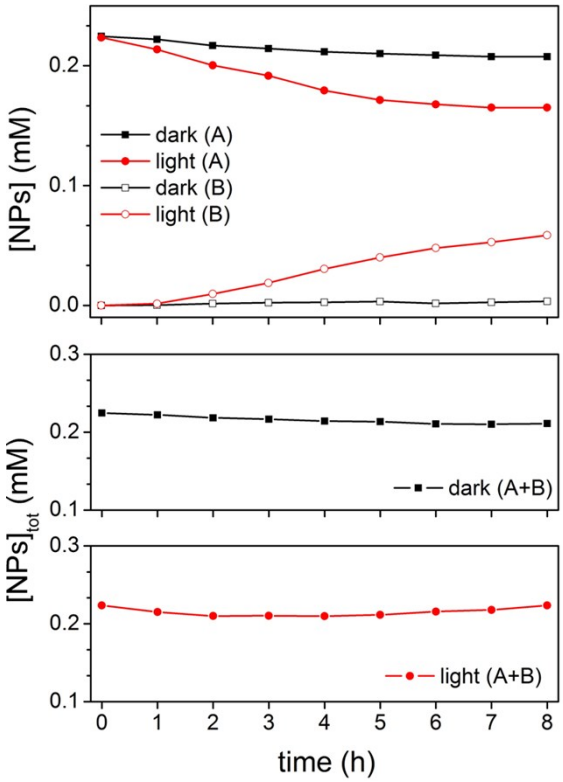

Figure S4. Upper panel: kinetics of polystyrene nanosphere diffusion in the presence of N719, measured in the dark (black plots) and under 532 nm irradiation (red plots). Middle and lower panels: total (side A + side B) nanosphere concentration measured in the dark and under light, respectively.

Figure S5

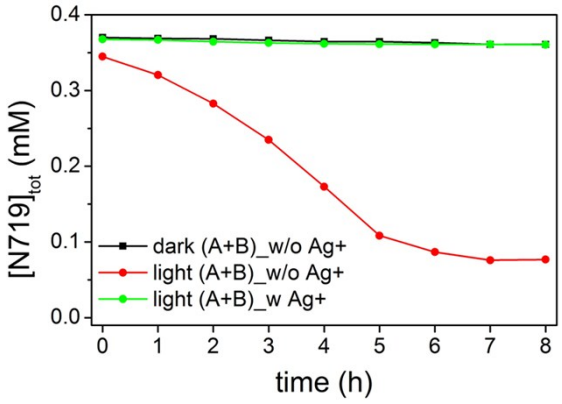

Figure S5. $[NPs]_t/[NPs]_0$ trends measured (in chamber A) under dark and in the presence of N719 dye (black plot), under 532 nm light and in the presence of N719 (red plot), and under 532 nm light with no N719 (green plot).

Figure S6

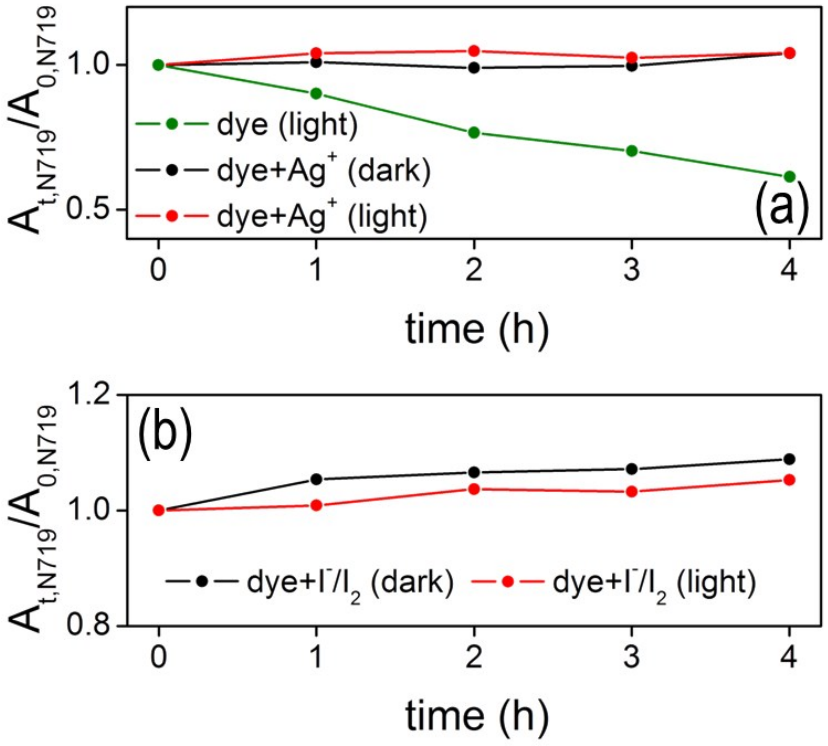

Figure S6. Control experiments carried out using TiO_2 NT arrays, that is, tube layers attached on Ti metal foils, in order to exclude any contribution from flow-through processes. (a) N719 A_t/A_0 trends measured in the dark and with Ag^+ ions (black plot), under 532 nm irradiation with Ag^+ ions (red plot) and under 532 nm irradiation with no Ag^+ ions (green plot). (b) N719 A_t/A_0 trends measured in the dark and with I^-/I_2 redox couple (black plot), under 532 nm irradiation with I^-/I_2 redox couple (red plot).

References

1 S. So, K. Lee and P. Schmuki, *J. Am. Chem. Soc.*, 2012, **134**, 11316–11318.
2 S. So, K. Lee and P. Schmuki, *Chem. - A Eur. J.*, 2013, **19**, 2966–2970.
3 J.-F. J.-F. Vanhumbeeck and J. Proost, *Corros. Rev.*, 2009, **27**, 117–204.
4 S. So, I. Hwang, F. Riboni, J. E. Yoo and P. Schmuki, *Electrochem. commun.*, 2016, **71**, 73–78.
5 N. Liu, H. Mirabolghasemi, K. Lee, S. P. Albu, A. Tighineanu, M. Altomare and P. Schmuki, *Faraday Discuss.*, 2013, **164**, 107.
6 S. P. Albu, A. Ghicov, S. Aldabergenova, P. Drechsel, D. LeClere, G. E. Thompson, J. M. Macak and P. Schmuki, *Adv. Mater.*, 2008, **20**, 4135–4139.
7 S. So, I. Hwang and P. Schmuki, *Energy Environ. Sci.*, 2015, **8**, 849–854.
8 M. K. Nazeeruddin, a Kay, E. Miiller, P. Liska, N. Vlachopoulos, M. Gratzel, C.-Lausanne and R. April, *J. Am. Chem. Soc.*, 1993, **115**, 6382–6390.
9 M. K. Nazeeruddin, S. M. Zakeeruddin, R. Humphry-Baker, M. Jirousek, P. Liska, N. Vlachopoulos, V. Shklover, C.-H. Fischer and M. Grätzel, *Inorg. Chem.*, 1999, **38**, 6298–6305.
10 T. a Heimer, E. J. Heilweil, C. a. Bignozzi and G. J. Meyer, *J. Phys. Chem. A*, 2000, **104**, 4256–4262.
11 S. a. Haque, Y. Tachibana, D. R. Klug and J. R. Durrant, *J. Phys. Chem. B*, 1998, **102**, 1745–1749.
12 F. Nour-Mohhamadi, S. D. Nguyen, G. Boschloo, A. Hagfeldt and T. Lund, *J. Phys. Chem. B*, 2005, **109**, 22413–22419.
13 F. De Angelis, S. Fantacci, E. Mosconi, M. K. Nazeeruddin and M. Grätzel, *J. Phys. Chem. C*, 2011, **115**, 8825–8831.
14 M. Grätzel, *Nature*, 2001, **414**, 338–344.
15 X. Wang, Y. Wang, H. Sui, X. Zhang, H. Su, W. Cheng, X. X. Han and B. Zhao, *J. Phys. Chem. C*, 2016, **120**, 13078–13086.
16 H. W. Roesky, J. Schimkowiak, K. Meyer-Bäse and P. G. Jones, *Angew. Chemie Int. Ed. English*, 1986, **25**, 1006–1007.
17 A. Hagfeldt, G. Boschloo, L. Sun, L. Kloo and H. Pettersson, *Chem. Rev.*, 2010, **110**, 6595–6663.
18 H. Hada, Y. Yonezawa and M. Saikawa, *Bull. Chem. Soc. Jpn.*, 1982, 55, 2010–2014.
19 B. Ohtani and S. Nishimoto, *J. Phys. Chem.*, 1993, **97**, 920–926.
20 Y. Tachibana, J. E. Moser, M. Grätzel, D. R. Klug and J. R. Durrant, *J. Phys. Chem.*, 1996, **100**, 20056–20062.
21 I. Paramasivam, J. M. Macak and P. Schmuki, *Electrochem. commun.*, 2008, **10**, 71–75.
22 J. M. Gardner, M. Abrahamsson, B. H. Farnum and G. J. Meyer, *J. Am. Chem. Soc*, 2009, **131**, 16206–16214.